Brownian ratchet for directional nanoparticle transport by repetitive stretch-relaxation of DNA

Inrok Oh,[1] Jeongeun Song,[2] Hye Ree Hyun,[2] Sang Hak Lee,[3] and Jun Soo Kim[2,*]

[1]*LG Chem Ltd, LG Science Park, Seoul 07796, Republic of Korea*

[2]*Department of Chemistry and Nanoscience, Ewha Womans University, Seoul 03760, Republic of Korea*

[3]*Department of Chemistry, Pusan National University, Busan 46241, Republic of Korea*

(Received 11 March 2022; revised 28 July 2022; accepted 13 October 2022; published 7 November 2022)

Brownian motion subject to a periodic and asymmetric potential can be biased by external, nonequilibrium fluctuations, leading to directional movement of Brownian particles. Sequence-dependent flexibility variation along double-stranded DNA has been proposed as a tool to develop periodic and asymmetric potentials for DNA binding of cationic nanoparticles with sizes below tens of nanometers. Here, we propose that repetitive stretching and relaxation of a long, double-stranded DNA molecule with periodic flexibility gradient can induce nonequilibrium fluctuations that tune the amplitude of asymmetric potentials for DNA-nanoparticle binding to result in directional transport of nanometer-sized particles along DNA. Realization of the proposed Brownian ratchet was proven by Brownian dynamics simulations of coarse-grained models of a single, long DNA molecule with flexibility variation and a cationic nanoparticle.

DOI: 10.1103/PhysRevE.106.054117

I. INTRODUCTION

A Brownian ratchet is a device that rectifies random Brownian motion and generates directed motion of Brownian particles [1–4]. One possible realization requires a Brownian particle to be subject to a periodic and asymmetric potential and under nonequilibrium fluctuations. Early Brownian ratchets utilized dielectrophoretic and optical forces to develop periodic and asymmetric potentials [5–7]. However, these forces do not provide effective asymmetric potentials for small particles below hundreds of nanometers. Although extensive efforts have been made for more than two decades [8–15], the size limit of Brownian ratchet has not been easily overcome, except for a recent work in which particles with sizes of tens of nanometers were transported directionally [16].

More recently, a new method to develop a periodic and asymmetric potential was proposed based on sequence-dependent flexibility variation of double-stranded DNA [17]. In this method, a periodic and asymmetric potential was set by the binding of a cationic nanoparticle (NP) to a DNA sequence with periodic variation of sequence-dependent flexibility. Driven by the strong electrostatic interactions between the DNA and NP against the sequence-dependent elastic energy of sharp DNA bending, the periodic and asymmetric potential was effective for particles with sizes even below tens of nanometers [18].

Here, we propose that single-molecule manipulation of DNA conformations by repetitive stretching and relaxation can be used as a source of nonequilibrium fluctuations to promote directional movement of a cationic NP with a size of several nanometers along DNA with periodic flexibility gradients. Repetitive stretching and relaxation of a single DNA molecule is routinely performed in experiments by varying the laser intensity in the optical tweezer, exerting strong and weak pulling forces (i.e., intensity modulation mode) to the colloidal sphere linked to the DNA molecule [19–21].

Realization of the proposed Brownian ratchet is demonstrated by performing Brownian dynamics (BD) simulations of models of a double-stranded DNA molecule and a cationic NP. A double-stranded DNA is modeled by a semiflexible polymer chain with periodic and asymmetric flexibility variation, which results in a periodic and asymmetric potential energy for binding with a cationic NP. We show that the amplitude of the periodic and asymmetric potential energy for DNA-NP binding can be tuned by varying the DNA extension. Then, by repeating coupled processes of stretching and relaxation of DNA bound with a cationic NP, we show that the repetitive DNA stretching and relaxation can promote the directional movement of a cationic NP along DNA with a periodic and asymmetric flexibility variation.

II. PROPOSED MECHANISM OF A BROWNIAN RATCHET

Imagine that one end of a double-stranded DNA is anchored to a substrate and the other end is linked to a colloidal particle constrained by an optical tweezer [Fig. 1(a)]. A cationic NP is bound to the negatively charged DNA by electrostatic attractions. The sequence of a long DNA molecule is designed such that the DNA molecule has a periodic and asymmetric flexibility variation, as shown in Fig. 1(b). It has been shown that the DNA flexibility varies with the sequence of nucleotides in double-stranded DNA [22–26]. A DNA fragment of a given length is designed to have a gradual and asymmetric variation of flexibility (referred to as the "flexibility gradient"). The sequence of this fragment was adopted from our previous work [17], which was composed of 64 DNA monomers with the gradual variation of flexibility in both directions. The length of this fragment with the

*jkim@ewha.ac.kr

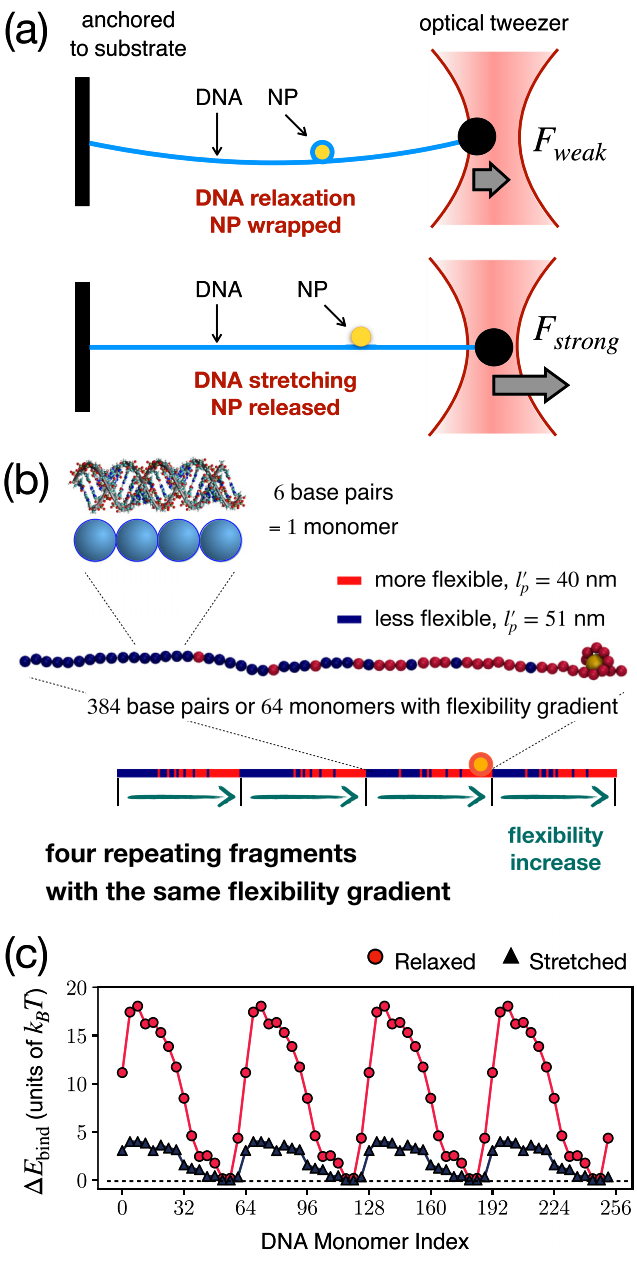

FIG. 1. (a) Schematic of the DNA stretch-relaxation Brownian ratchet. (b) A layout for a long DNA molecule consisting of four repeating fragments of the same flexibility gradient. The DNA molecule is modeled as a semiflexible polymer chain and each DNA monomer represents six base pairs with different local flexibilities of $l_p' = 40$ nm and of $l_p' = 51$ nm for more and less flexible DNA regions, respectively. Each fragment with the flexibility gradient is composed of 64 DNA monomers, in which the local flexibility increases from one end to the other by arranging DNA monomers with different local flexibilities. A single, long DNA molecule is synthesized by repeating the sequence with the same flexibility gradient four times. (c) Relative variation of the potential energy for DNA-NP binding, ΔE_{bind}. The circular and triangular symbols represent the data for relaxed and stretched DNA conformations induced by weak and strong pulling forces, respectively. This periodic and asymmetric potential energy was built by duplicating the asymmetric potential energy of a single DNA fragment presented in Fig. 2.

flexibility gradient is defined as L_0 and used as a unit of DNA length. This fragment with the flexibility gradient is synthesized repetitively to form a single, long DNA molecule with a periodic and asymmetric flexibility variation, as shown in Fig. 1(b).

When a cationic NP binds to the DNA, strong electrostatic attractions induce DNA to wrap around the NP. Due to the high energy cost for sharp DNA bending, the potential energy for DNA wrapping around the NP varies sensitively depending on the DNA flexibility. Since the DNA molecule has a periodic and asymmetric flexibility variation, the NP experiences the periodic and asymmetric potential energy for DNA binding and wrapping, as shown in Fig. 1(c). In the figure, the asymmetric potential energy decreases from left to right on each DNA fragment, suggesting that the DNA flexibility increases from left to right in each DNA fragment.

DNA conformations can be relaxed or stretched depending on the strength of the pulling force exerted by the optical tweezer to the DNA-linked colloidal particle, as depicted in Fig. 1(a). When the DNA is relaxed by applying a weak pulling force, the NP is wrapped completely around by the DNA, which results in the strongly asymmetric potential energy for DNA-NP binding. As a result, the location of the NP is biased asymmetrically toward the more flexible DNA region where the potential energy is minimal. On the other hand, when the DNA is stretched by applying a strong pulling force, the DNA wrapping around a NP is disrupted by strong DNA tension and the NP remains bound to the DNA without significant DNA bending. This results in a significant reduction of the potential energy for DNA-NP binding, as shown in Fig. 1(c), thus facilitating diffusive movement of a NP along the DNA. These qualitative descriptions of the effect of DNA stretching and relaxation on the NP position and movement will be demonstrated below in Figs. 2 and 3.

In a coupled process of DNA stretching and relaxation, it is probable that the NP bound to the DNA can move along DNA to the right in the direction of the DNA flexibility gradient. After diffusive movements in the stretched DNA state, the NP in the subsequent relaxed DNA state is forced to be positioned at a minimum of the asymmetric potential energy again. If the NP has remained within the original DNA fragment during the diffusive movements, the NP is subject to the asymmetric potential of the same DNA fragment as in the previous relaxed DNA state and moves back to the same minimum energy position, resulting in no net displacement. However, if the NP has moved to a neighboring DNA fragment by diffusive movements in the stretched DNA state, the NP is then subject to an asymmetric potential of the new DNA fragment in the subsequent relaxed DNA state. In this case, it moves to the minimal energy position of the new DNA fragment, resulting in a net displacement of the NP by the length of a DNA fragment. However, such movement of a NP to neighboring DNA fragments is asymmetric because the starting NP position in the stretched DNA state is biased to the right on each DNA fragment. As a result, in a couple process of DNA stretching and relaxation, the NP either remains in the same position within the original DNA fragment or moves to the right in the direction of the DNA flexibility gradient. By repeating a series

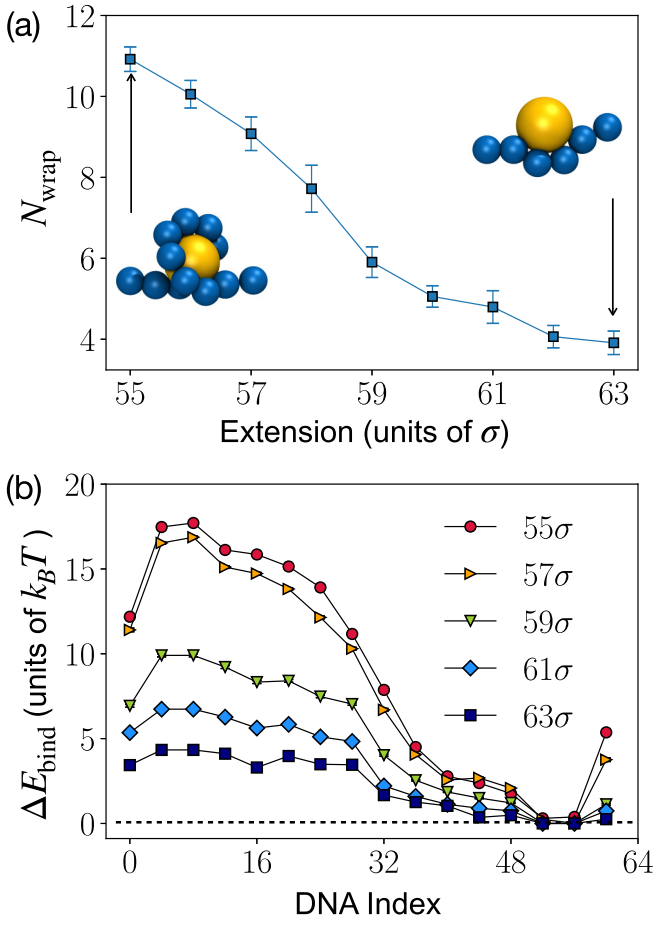

FIG. 2. (a) Number of DNA monomers wrapping around a cationic NP, N_{wrap}, as a function of the DNA extension. (b) Relative variation of the potential energy for DNA-NP binding, ΔE_{bind}, at each DNA extension as a function of the DNA index along a flexibility gradient. Error bars are smaller than the symbols. The DNA index in the figure corresponds to that of the central DNA monomer in the wrapping structure of the DNA-NP complex.

of the coupled processes of DNA stretching and relaxation, a NP is anticipated to move, on average, to the right along the flexibility gradient.

III. SIMULATION MODELS AND METHODS

A. Computational models

A double-stranded DNA molecule was modeled by a semiflexible polymer chain with its size, charge, and flexibility consistent with those of double-stranded DNA [17,18]. Each group of six base pairs in the DNA double helix was modeled by a single spherical bead with diameter of $\sigma = 2$ nm and an electric charge of $-12e$, where e is the elementary charge. The diameter of DNA monomers, σ, was used as a unit of length in this work. DNA monomers were connected to each other into a single polymer chain by a combination of a repulsive part of the Lennard-Jones (LJ) potential energy, U_r, and finite extension nonlinear elastic (FENE) potential energy, U_f:

$$U_r(r) = \begin{cases} 4\epsilon_{LJ}\left[\left(\frac{\sigma}{r}\right)^{12} - \left(\frac{\sigma}{r}\right)^{6}\right] + \epsilon_{LJ}, & 0 < r < 2^{1/6}\sigma, \\ 0 & \text{elsewhere} \end{cases} \quad (1)$$

and

$$U_f(r) = -\tfrac{1}{2}k_f R_f^2 \ln[1 - (r/R_f)^2]. \quad (2)$$

Here, r is the distance between a pair of consecutive DNA monomers and $\epsilon_{LJ} = 1k_BT$, where k_B is the Boltzmann constant and T is temperature. In addition, $k_f = 30k_BT/\sigma^2$ and $R_f = 1.5\sigma$, which were chosen to prevent bond crossing [27]. Sequence-dependent DNA flexibility was modeled by the harmonic restraint, U_θ, on the angle defined for each triple of consecutive DNA monomers:

$$U_\theta(\theta) = \frac{k_\theta}{2}\theta^2. \quad (3)$$

θ is the angle between two consecutive bond vectors, $\vec{b}_{i,i+1}$ and $\vec{b}_{i+1,i+2}$, of monomers i, $i+1$, and $i+2$. The flexibility of a polymer chain is quantitatively described in terms of the persistence length, which is a measure of the polymer rigidity or the inverse of flexibility. The local DNA persistence length was reported to range between 40 and 55 nm for double-stranded DNA [22]. In this work, two values of k_θ were used to represent more and less flexible DNA regions, $k_\theta = 18k_BT/\text{rad}^2$ and $24k_BT/\text{rad}^2$, which correspond to more and less flexible DNA regions with local persistence lengths, l_p', of 40 nm and 51 nm, respectively [18]. Nonbonded interactions between DNA monomers were described by the excluded volume interaction and electrostatic repulsion. The excluded volume interaction was modeled by the repulsive LJ potential energy, U_r, which is the same as Eq. (1), and the electrostatic interaction was represented by the Debye-Hückel potential energy, U_{DH},

$$U_{DH} = \frac{l_B z_m^2 k_B T}{(1 + \kappa\sigma/2)^2}\frac{\exp[-\kappa(r-\sigma)]}{r}. \quad (4)$$

Here, $z_m = -12$ is the charge number of DNA monomers and l_B is the Bjerrum length defined as $e^2/(4\pi\epsilon_0\epsilon_r k_B T) \approx 0.71$ nm in pure water at 298 K, in which ϵ_0 is the vacuum permittivity and ϵ_r is the relative dielectric constant in pure water. κ is the inverse Debye length expressed as $\kappa \approx (8\pi l_B N_A c_{\text{salt}})^{1/2}$ in a dilute DNA and NP solution. c_{salt} is the concentration of monovalent salt, N_A is Avogadro's number, and, assuming $c_{\text{salt}} = 0.145$ M, $\kappa^{-1} = 0.80$ nm in this work.

A cationic NP was modeled as a spherical particle with a diameter of 4 nm (or 2σ) and an electric charge of $+64e$ [18]. The interactions of a NP with DNA monomers were also described by the repulsive LJ potential energy, U_r, and the Debye-Hückel potential energy, U_{DH}:

$$U_r(r) = \begin{cases} 4\epsilon_{LJ}\left[\left(\frac{\sigma}{r-r_0}\right)^{12} - \left(\frac{\sigma}{r-r_0}\right)^{6}\right] + \epsilon_{LJ}, & 0 < r - r_0 < 2^{1/6}\sigma, \\ 0 & \text{elsewhere.} \end{cases} \quad (5)$$

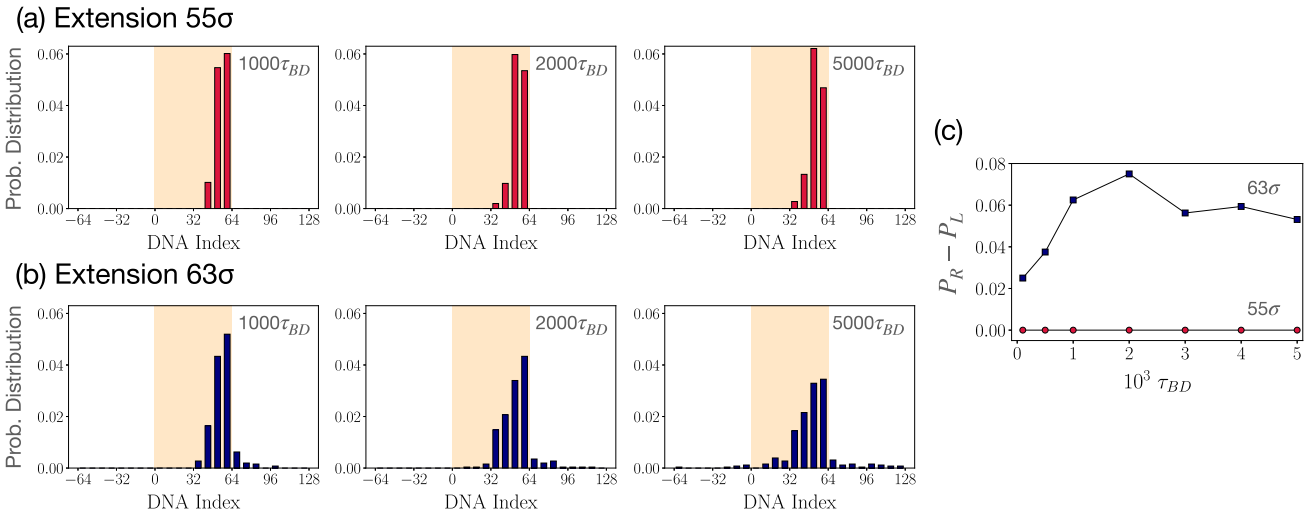

FIG. 3. (a), (b) Probability distributions of the NP position along DNA after several time durations for DNA extensions of 55σ and 63σ, respectively. Initially, the NP was placed in the more flexible region of a DNA fragment with the index number of 60. The simulations were repeated 320 times to calculate the probability distributions. The orange-colored region in the figure indicates the DNA fragment where the NP was initially placed. The neighboring DNA fragments on the right and left were indicated by the DNA indices >64 and $\leqslant 0$, respectively. (c) The probability of net displacement to the right, calculated by $P_R - P_L$, where P_R and P_L are the probabilities for an NP to move to the right (to the region with the DNA indices of >64) and to the left (with the DNA indices of $\leqslant 0$), respectively.

Here, r_0 is the shift of the potential energy to account for the larger size of the NP and was set to a value of $\sigma/2$:

$$U_{DH} = \frac{l_B z_p z_m k_B T}{(1+\kappa\sigma_p/2)(1+\kappa\sigma_m/2)} \frac{\exp\{-\kappa[r-(\sigma_p+\sigma_m)/2]\}}{r}. \tag{6}$$

$z_p = +64$ and $z_m = -12$ are the charge numbers and $\sigma_p = 2\sigma$ and $\sigma_m = \sigma$ are the diameters of the NP and DNA monomers, respectively.

In this work, the effects of water molecules and monovalent ions were implicitly included by using the Debye-Hückel potential energy in Eqs. (4) and (6). If water molecules and ions were included explicitly in the simulations, some of them would come between DNA and NP resulting in obstructing the sliding and rolling dynamics of the NP along DNA. Nevertheless, the average behavior of sliding and rolling dynamics of the NP along DNA is expected to be the same despite the time delay in simulations unless the ion concentration is too high. Simulation studies using more detailed models with explicit presence of water molecules and ions are in progress. So far, these studies confirmed that a small difference in the DNA persistence length results in qualitative and quantitative differences in the complex formation between DNA and NP [25,26].

B. BD simulation method

BD simulations were performed using GROMACS v. 4.5.4 [28]. The BD simulation method was used to describe the solvent-induced Brownian motions of particles without the explicit presence of solvent molecules and was performed by solving the position Langevin equation in Eq. (7) [29]. Hydrodynamic interactions were not considered in this work. In each time step Δt, particles were displaced from a previous position $\vec{r}(t)$ at time t to an updated position $\vec{r}(t+\Delta t)$:

$$\vec{r}(t+\Delta t) = \vec{r}(t) + \frac{D_0 \vec{F}(t)}{k_B T}\Delta t + \vec{R}(\Delta t). \tag{7}$$

Here, D_0 is the diffusion coefficient of each particle in pure solvent, $\vec{F}(t)$ is the total force acting on the particle (calculated from bonded and nonbonded interactions, as described above), and $\vec{R}(\Delta t)$ is a random displacement with a Gaussian distribution function with a zero mean and variance of $6D_0\Delta t$. The value of D_0 for DNA monomers is twice as large as that for the NP. The time scale for the Brownian motion of DNA monomers, $\tau_{BD} = \sigma^2/D_0$, was used as a unit of time in this work, which is roughly the average time for a DNA monomer to move a distance of its own size σ. A time step of $\Delta t = 10^{-4}\,\tau_{BD}$ was used for all simulations. The diffusion coefficients of DNA oligomers with 20 or 21 base pairs in aqueous solutions were reported to be 1.2×10^{-6} or 5.3×10^{-7} cm^2/s, respectively [30,31]. Assuming the size of 6.8 nm (the contour length of 20-base pair DNA), τ_{BD} is estimated to be 0.39 or 0.87 μs. Since DNA monomers used in our simulation have a shorter length of six base pairs, the diffusion coefficient and size are expected to be different. Thus we consider that the time unit, τ_{BD}, is roughly in the range of 0.01–0.1 μs.

To confirm the possible realization of the proposed Brownian ratchet, we performed two sets of the BD simulations. The first set of simulations was performed to determine the structures of a DNA-NP complex and the distributions of the NP over a DNA fragment with the flexibility gradient at each desired value of DNA extensions, as shown in Figs. 2 and 3. In this case, the size of the simulation box was set to the DNA extension and a single DNA fragment with the flexibility gradient was stretched across the simulation box. The periodic boundary condition was applied to mimic a long

DNA molecule with repeated sequences of the DNA fragment. To obtain an ensemble of a DNA-NP complex used in Fig. 2, a NP was placed at one of the eight equally spaced positions on a DNA fragment and a total duration of $2000\tau_{BD}$ was run for each DNA extension. For each initial position, the simulations were repeated 40 times, resulting in a total of 320 simulation trajectories. To calculate the probability distributions of a NP along DNA presented in Fig. 3, a NP was placed in the more flexible DNA region and 320 independent simulations were performed for a time duration of $5000\tau_{BD}$.

The second set of simulations was performed to investigate the directional movement of a NP along the DNA, as shown in Fig. 6. A long DNA molecule composed of four DNA fragments with the same flexibility gradient was stretched to the desired value of the DNA extension, as shown in Fig. 1(b). A NP was placed at the leftmost part of the DNA and its movement over the cycles of DNA stretching and relaxation was tracked. For each trajectory of the NP movement, we performed 300 cycles of DNA stretching, intermediate pause, and relaxation between the DNA extensions of 239σ and 252σ, as shown in Fig. 5. The simulation durations for DNA stretching and relaxation were $1300\tau_{BD}$ and that for the intermediate pause was $1000\tau_{BD}$. To obtain the average behavior, we performed 32 independent simulations of the 300 cycles.

IV. RESULTS AND DISCUSSION

A. Tuning the asymmetric potential energy by DNA extension

The first step to prove the proposed mechanism of a Brownian ratchet is to demonstrate the modulating effect of the DNA extension on the asymmetric potential energy associated with the formation of a DNA-NP complex. For this purpose, we generated 320 representative structures of a DNA-NP complex at each DNA extension, as described in Sec. III. The simulations were performed at a fixed DNA extension between 55σ and 63σ, corresponding to the most relaxed and most stretched DNA conformational states under investigation, respectively. In Fig. 2(a), different DNA-NP structures were quantified in terms of the number of DNA monomers wrapping around the NP, N_{wrap}. When the distance of a DNA monomer to the NP is less than the critical distance, the DNA monomer is considered to wrap around the NP and counted for N_{wrap}. The critical distance was set to 1.8σ based on the radial distribution function of DNA monomers around the NP in the DNA-NP complexes (data not shown). The value of N_{wrap} decreases as the DNA extension increases. At highly stretched DNA extensions of $\geqslant 62\sigma$, the NP is bound to only about four DNA monomers and the extent of DNA bending is not very large (as shown in the snapshot of the complex for the extension of 63σ). On the other hand, at relaxed DNA extensions of $\leqslant 57\sigma$, the NP is wrapped around by 9 to 11 DNA monomers, suggesting sharp DNA bending around the NP.

In accordance with the structural transition, the potential energy of DNA-NP binding, ΔE_{bind}, also varies with the DNA extension. The potential energy is presented in Fig. 2(b) as a function of the index number of DNA monomers along the flexibility gradient. By assuming that the DNA-NP complex has a fixed structure, all bonding and nonbonding interaction terms, except for the bending energy, cancel out along the DNA fragment and, thus, the potential energy is solely dependent on the angular bending energy of DNA along the DNA fragment with a flexibility gradient. Therefore, the potential energy decreases asymmetrically from left to right on each DNA fragment as the DNA flexibility increases. For DNA extensions of $\leqslant 57\sigma$, the asymmetric variation in the potential energy is the most marked because the DNA is sharply bent to wrap around the NP. On the other hand, for long DNA extensions of $\geqslant 62\sigma$, the DNA is only partially bent in the DNA-NP complex and, therefore, the potential energy is very weakly asymmetric along the DNA. It is noted that the DNA-NP structure may vary over the flexibility gradient and the assumption of the fixed structure could have overestimated the potential energy. Nevertheless, it is clear that the asymmetric potential energy can be modulated by varying the DNA extension.

Due to the asymmetry in the potential energy for DNA-NP binding, the probability distribution of a cationic NP along the DNA is also asymmetric, as shown in Figs. 3(a) and 3(b). However, the comparison of the probability distributions reveals that the asymmetry in the probability distribution is also modulated by the DNA extension. The probability distributions in Figs. 3(a) and 3(b) were determined from the BD simulations at DNA extensions of 55σ and 63σ at several time durations of $t = 100\tau_{BD}$–$5000\tau_{BD}$. In each fragment of 64 DNA monomers, the NP was initially placed in the more flexible region specified by the DNA index of 60, and after each time duration the NP location was determined. The simulation was repeated 320 times to determine the probability distribution of the NP location. Placed in the more flexible DNA region with lower potential energy, a NP is likely to remain in the same region [17,18,25,26], as shown in Figs. 3(a) and 3(b), leading to the localization of a NP in more flexible regions. However, as is the case with the asymmetric potential energy, the asymmetry in the probability distributions is also diminished by DNA stretching from 55σ to 63σ. Accordingly, at the extension of 63σ, the movement of a NP along DNA becomes more facile to the less flexible DNA regions, as can be seen by nonzero probability distributions in the less flexible regions (indicated by the DNA indices of either <32 or >64) in Fig. 3(b). Strict localization of a NP at the DNA extension of 55σ and more facile NP movement at 63σ can also be confirmed by the calculation of the mean square displacement (MSD) of a NP along the DNA, as shown in Fig. 4. The slope of the MSD is significantly larger at the DNA extension of 63σ than at the extension of 55σ, suggesting that the diffusive movement of a NP is further facilitated by DNA stretching.

The efficiency of the Brownian ratchet mechanism proposed in Sec. II is largely determined by the durations for stretched and relaxed DNA conformations. The duration for DNA relaxation is required to be long enough to localize the NP in the more flexible region of the DNA fragment. On the other hand, the duration for DNA stretching needs to be optimized for asymmetric movement of the NP along DNA: it is required to be long enough to allow the NP, located initially in the more flexible region, to diffuse to the neighboring DNA fragment close to the starting location but not long enough to allow the NP diffusion to the neighboring DNA fragment

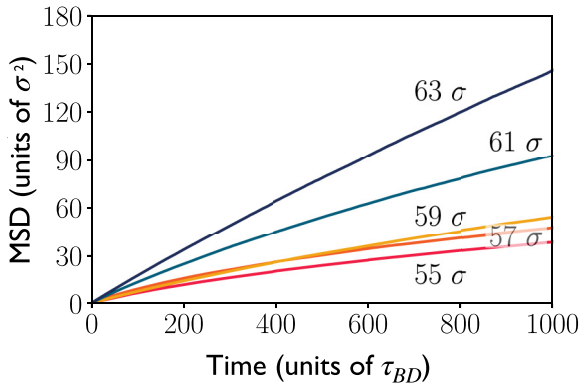

FIG. 4. Mean squared displacement (MSD) of a NP along DNA, in units of σ^2, at different DNA extensions between 55σ and 63σ.

on the opposite side. Therefore, we determined the optimal durations for stretched and relaxed DNA conformations for the effective Brownian ratchet, as shown in Fig. 3(c).

The probability distributions in Fig. 3(a) were obtained for the DNA extension of 55σ and show that the NP initially located in the more flexible region with the DNA index of 60 remained in the more flexible DNA region (with the DNA indices between 32 and 64) without moving to the neighboring DNA fragment after time durations of $t = 1000\tau_{BD}$–$5000\tau_{BD}$. On the other hand, the probability distributions in Fig. 3(b) obtained for the DNA extension of 63σ show that there is a chance that a NP moves to the neighboring DNA fragment on the right (specified by the DNA indices >64). The NP movement to the neighboring DNA fragment on the left (with the DNA indices of $\leqslant$0) has not been observed at time durations of $1000\tau_{BD}$–$2000\tau_{BD}$, whereas it was observed after the time duration of $5000\tau_{BD}$. The net displacement to the right along DNA can be predicted by calculating the probabilities of NP movements to the DNA fragments on the right, P_R, and to the left, P_L. The difference $P_{net} = P_R - P_L$ predicts the probability of the effective NP displacement to the DNA fragment on the right. In Fig. 3(c), P_{net} is depicted at various time durations and it is seen that the net displacement to the right at the DNA extension of 63σ is most probable with the optimal time duration of $t = 2000\tau_{BD}$. On the other hand, $P_{net} = 0$ at the DNA extension of 55σ, confirming that the NP remains in the same flexible DNA region over the time durations. Therefore, it is concluded that the optimal time duration for effective NP displacement is $t = 2000\tau_{BD}$ at the DNA extension of 63σ, whereas any time duration over $t = 1000\tau_{BD}$ suffices at the extension of 55σ.

B. Repetitive DNA stretching and relaxation for directional NP transport

Based on the confirmation that the variation of the DNA extension results in dramatic changes of the asymmetric potential energy for DNA-NP binding and the NP diffusion over DNA, the Brownian ratchet was demonstrated directly by performing BD simulations for the cycles of DNA stretching and relaxation. The DNA molecule was composed of four consecutive fragments with the same flexibility gradient, as shown in Fig. 1(b). Each DNA fragment contained 64 DNA

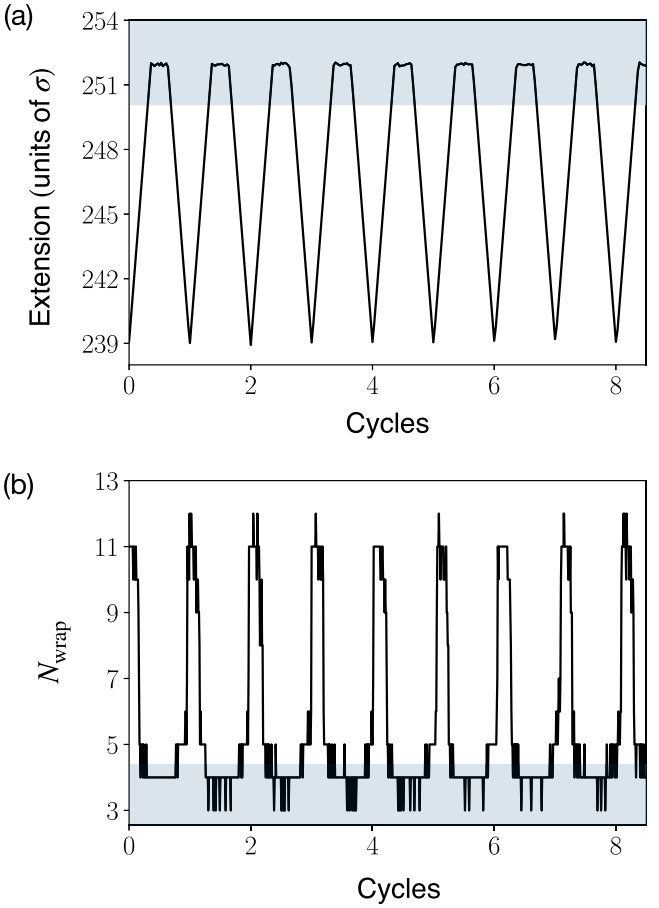

FIG. 5. (a) Cycles of DNA stretching, intermediate pause, and relaxation were repeated for a single, long DNA molecule composed of four consecutive DNA fragments with the same flexibility gradient. Only a subset of 300 cycles in a single simulation was presented in the figure. (b) The corresponding change of N_{wrap}. The stretched DNA states are indicated by the gray shaded area ($N_{\text{wrap}} \leqslant 4$) in both figures. The time duration for the stretched DNA states ($N_{\text{wrap}} \leqslant 4$) was estimated to be 1843 ($\pm$61) τ_{BD} and the average value of N_{wrap} when $N_{\text{wrap}} \leqslant 4$ was 3.95 ($\pm$0.22).

monomers and, thus, the contour length of the DNA molecule was 256σ. We assumed that the flexibility in each DNA fragment increases from left to right. A NP was initially placed at the leftmost part of the DNA, which is the least flexible DNA region of the first DNA fragment, and its position was tracked over repetitive DNA stretching and relaxation to confirm the directed motion of a NP.

Nonequilibrium fluctuations required for the Brownian ratchet were introduced by repetitive DNA stretching and relaxation within the range of DNA extensions of 239σ and 252σ, as shown in Fig. 5. A cycle begins with DNA stretching from 239σ to 252σ with a rate of $0.01\sigma/\tau_{BD}$ for a duration of $1300\tau_{BD}$. Then, the additional BD simulation is performed at the constant DNA extension of 252σ for a time duration of $1000\tau_{BD}$ to ensure the diffusive movement of a NP in the stretched DNA state. Finally, the DNA is slowly relaxed by gradually decreasing the extension to 239σ with a rate of $0.01\sigma/\tau_{BD}$ for a duration of $1300\tau_{BD}$. Therefore, a cycle of DNA stretching, intermediate pause, and relaxation occurs for

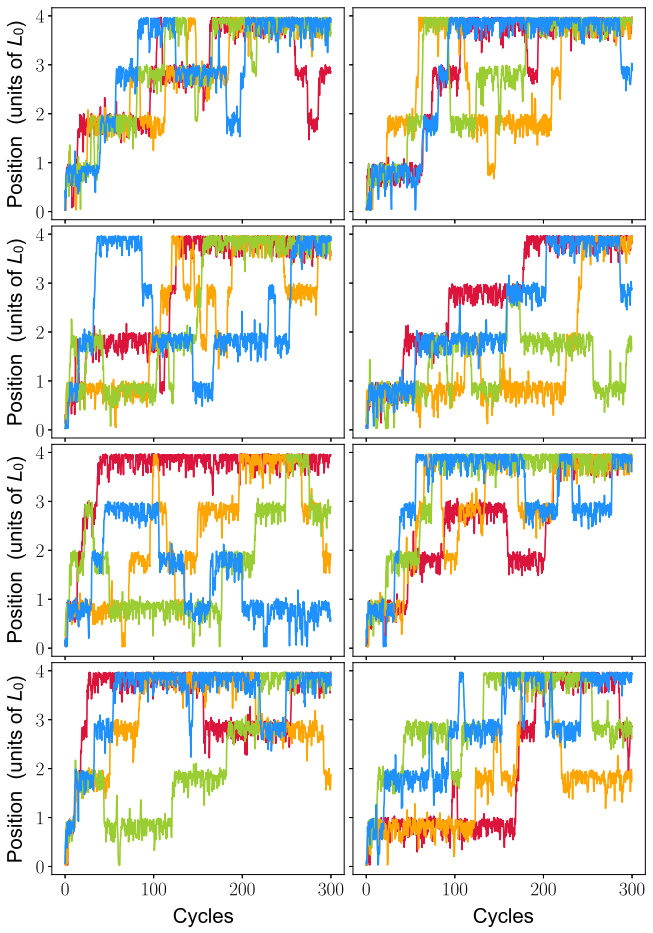

FIG. 6. Processive NP movement along DNA from a total of 32 independent simulation trajectories grouped into eight subfigures for visual clarity. Each trajectory was obtained from 300 cycles of DNA stretching and relaxation. The x axis is the number of the cycles composed of DNA stretching, intermediate pause, and relaxation. The y axis represents the NP position in units of the length of a single DNA fragment (L_0) and the initial NP position is indicated by the value of 0.

a duration of $3600\tau_{BD}$. For a set of DNA and a NP, 300 cycles of DNA stretching and relaxation were repeated to investigate directional NP movement.

The range of the DNA extension between 239σ and 252σ was chosen based on the degree of DNA wrapping around the NP. The number of DNA monomers wrapping around the NP, N_{wrap}, ranges between 3 and 12, as shown in Fig. 5(b), which is consistent with the range of the DNA wrapping calculated for a single DNA fragment in Fig. 2(a). We assume that DNA is in the stretched conformations when $N_{\text{wrap}} \leqslant 4$ because it corresponds to the DNA extension of $\geqslant 62\sigma$ for a single DNA fragment for which the diffusive movement of the NP is more facile with the steepest MSD in Fig. 4. The DNA state in the stretched conformations ($N_{\text{wrap}} \leqslant 4$) is shaded gray in Fig. 5(b) and, accordingly, in Fig. 5(a). The time duration of the stretched DNA state in each cycle was estimated to be 1843 (± 61) τ_{BD} and, thus, the remaining $\sim 1757\tau_{BD}$ corresponds to the relaxed DNA state. The time duration estimated for the stretched DNA state is similar to the optimal time duration of $2000\tau_{BD}$ for the efficient Brownian ratchet as shown in Fig. 3(c), while the time duration in the relaxed DNA state is sufficient with $\geqslant 1000\tau_{BD}$.

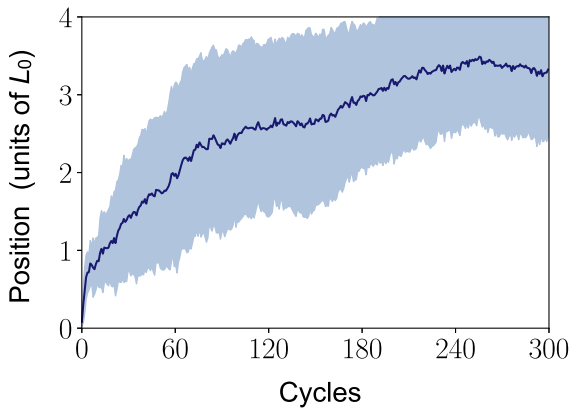

FIG. 7. Processive NP movement along DNA averaged over 32 simulation trajectories presented in Fig. 6. The y axis represents the average NP position in units of the length of a single DNA fragment (L_0) and the initial NP position is indicated by the value of 0. The thick plot in dark blue represents the average NP position, whereas the shaded area is the standard deviations over the cycles calculated from the 32 simulations.

The directional NP transport by the Brownian ratchet was proven by performing 32 independent simulations. The results from the 32 simulations are presented in Fig. 6. Four simulation results are plotted together in each subfigure for visual clarity. The y axis represents the NP position and the value from 0 to 4 corresponds to the number of DNA fragments over which the NP has moved from the left to right during 300 cycles. It is clear that the NP moves directionally to the rightmost end of the DNA molecule. There are a few simulation trajectories for which the NP returned to the initial location after 300 cycles of DNA stretching and relaxation. However, most trajectories show that the NP moved over more than a distance of three DNA fragments after 300 cycles. The average and standard deviation of the NP position over cycles is presented in Fig. 7. Therefore, this verifies the realization of the proposed Brownian ratchet based on the repetitive DNA stretching and relaxation.

V. CONCLUSIONS

We proposed a Brownian ratchet for directional transport of a cationic NP along a long, double-stranded DNA molecule operated by repetitive DNA stretching and relaxation. Along the DNA molecule with the periodic and asymmetric flexibility variation, the NP experiences a periodic and asymmetric potential for DNA-NP binding. We first showed that the DNA stretching and relaxation changes the amplitude of the asymmetry in the potential energy for DNA-NP binding. Then, the realization of the proposed Brownian ratchet was proven by BD simulations over a long DNA molecule with four repetitive flexibility gradients. We performed 32 independent simulations of 300 cycles of DNA stretching and relaxation. The simulation results suggest that a cationic NP can, on average, be transported in a specific direction along the DNA by repetitive DNA stretching and relaxation.

Recently, we proposed a Brownian ratchet for directional NP transport [17]. In the previous method, the periodic and asymmetric potential energy was generated by the same strategy using the flexibility variation of a long, double-stranded DNA molecule. However, nonequilibrium fluctuations required for Brownian ratcheting were induced by repetitive changes of the solution salt concentrations. In practice, this requires repetitive exchange of salt solutions with different concentrations, which is nontrivial at all to realize in experimental systems. On the other hand, in this work, we proposed nonequilibrium fluctuations by repetitive DNA stretching and relaxation, which is more straightforward because it is a routine process in single-molecule experiments in biophysics. Therefore, this Brownian ratchet based on the repetitive DNA stretching and relaxation is anticipated to be realized readily in future experiments.

This Brownian ratchet may be useful in future applications where the delivery of small nanoparticles over a long distance of several hundreds of nanometers is required. Assume that a long DNA molecule is linked between two separated sites on the same surface or on separate surfaces: one site is abundant with a large number of functional nanoparticles and the other requires them for any reaction or process. During an inactive period, the long DNA molecule serves as a nanoparticle reservoir in which nanoparticles remain bound sparsely to more flexible regions along relaxed DNA. When the nanoparticles are required for the reaction or process, the nanoparticles are processively delivered by repetitive stretching and relaxation of the DNA as proposed in this work. It is noted that the current form of the proposed Brownian ratchet is not efficient enough to be used in practical applications. However, the proposed model is a proof of concept and the efficiency may be improved in practical realization by designing an optimal DNA sequence with longer and more asymmetric flexibility gradient or by finding optimal time durations for DNA stretching and relaxation.

Rapid development of DNA nanotechnology has largely relied on increasing the capability of precise design of sequence-specific hybridization of complementary DNA strands and accurate synthesis of DNA sequences. On the other hand, the Brownian ratchet proposed in this work is based on the sequence-dependent DNA mechanics, which has rarely been exploited in DNA nanotechnology. The sequence-dependent DNA flexibility may not be very useful in manipulating structures of linear DNA molecules, which may be the reason for the lack of mechanics-based DNA nanotechnology. In this work, however, the sequence-dependent variation of DNA flexibility plays an important role in controlling the position of a cationic NP due to sharp DNA bending induced by complex formation with the NP. In the same way, it is also anticipated that the sequence-dependent DNA flexibility can be a useful tool in DNA nanotechnology when the structure formation involves sharp DNA bending [32–35].

ACKNOWLEDGMENTS

This research was supported by the National Research Foundation of Korea (NRF) under Grants No. NRF-2019R1A2C1084414 and No. NRF-2020R1A5A2019210.

[1] R. D. Astumian, Science **276**, 917 (1997).
[2] P. Reimann, Phys. Rep. **361**, 57 (2002).
[3] P. Hänggi and F. Marchesoni, Rev. Mod. Phys. **81**, 387 (2009).
[4] S. Erbas-Cakmak, D. A. Leigh, C. T. McTernan, and A. L. Nussbaumer, Chem. Rev. **115**, 10081 (2015).
[5] J. Rousselet, L. Salome, A. Ajdari, and J. Prost, Nature (London) **370**, 446 (1994).
[6] L. P. Faucheux, L. S. Bourdieu, P. D. Kaplan, and A. J. Libchaber, Phys. Rev. Lett. **74**, 1504 (1995).
[7] L. P. Faucheux and A. Libchaber, J. Chem. Soc. Faraday Trans. **91**, 3163 (1995).
[8] J. S. Bader, R. W. Hammond, S. A. Henck, M. W. Deem, G. A. McDermott, J. M. Bustillo, J. W. Simpson, G. T. Mulhern, and J. M. Rothberg, Proc. Natl. Acad. Sci. USA **96**, 13165 (1999).
[9] C. Marquet, A. Buguin, L. Talini, and P. Silberzan, Phys. Rev. Lett. **88**, 168301 (2002).
[10] S. Matthias and F. Müller, Nature (London) **424**, 53 (2003).
[11] S.-H. Lee, K. Ladavac, M. Polin, and D. G. Grier, Phys. Rev. Lett. **94**, 110601 (2005).
[12] L. Bogunovic, R. Eichhorn, J. Regtmeier, D. Anselmetti, and P. Reimann, Soft Matter **8**, 3900 (2012).
[13] D. Reguera, A. Luque, P. S. Burada, G. Schmid, J. M. Rubí, and P. Hänggi, Phys. Rev. Lett. **108**, 020604 (2012).
[14] S. Verleger, A. Grimm, C. Kreuter, H. M. Tan, J. A. van Kan, A. Erbe, E. Scheer, and J. R. C. van der Maarel, Lab Chip **12**, 1238 (2012).
[15] S.-H. Wu, N. Huang, E. Jaquay, and M. L. Povindelli, Nano Lett. **16**, 5261 (2016).
[16] M. J. Skaug, C. Schwemmer, S. Fringes, C. D. Rawlings, and A. W. Knoll, Science **359**, 1505 (2018).
[17] S. Park, J. Song, and J. S. Kim, Sci. Adv. **5**, eaav4943 (2019).
[18] S. Park, H. Joo, and J. S. Kim, Soft Matter **14**, 817 (2018).
[19] K. Svoboda and S. M. Block, Annu. Rev. Biophys. Biomol. Struct. **23**, 247 (1994).
[20] K. C. Neuman and S. M. Block, Rev. Sci. Instrum. **75**, 2787 (2004).
[21] A. Rohrbach, Phys. Rev. Lett. **95**, 168102 (2005).
[22] S. Geggier and A. Vologodskii, Proc. Natl. Acad. Sci. USA **107**, 15421 (2010).
[23] H.-M. Chuang, J. G. Reifenberger, H. Cao, and K. D. Dorfman, Phys. Rev. Lett. **119**, 227802 (2017).
[24] J. S. Mitchell, J. Glowacki, A. E. Grandchamp, R. S. Manning, and J. H. Maddocks, J. Chem. Theory Comput. **13**, 1539 (2017).
[25] S. Bae, I. Oh, J. Yoo, and J. S. Kim, ACS Omega **6**, 18728 (2021).
[26] S. Bae and J. S. Kim, J. Chem. Theory Comput. **17**, 7952 (2021).
[27] K. Kremer and G. S. Grest, J. Chem. Phys. **92**, 5057 (1990).
[28] B. Hess, C. Kutzner, D. van der Spoel, and E. Lindahl, J. Chem. Theory Comput. **4**, 435 (2008).
[29] D. L. Ermak and J. A. McCammon, J. Chem. Phys. **69**, 1352 (1978).

[30] N. C. Stellwagen, S. Magnusdottir, C. Gelfi, and P. G. Righetti, Biopolymers **58**, 390 (2001).
[31] G. L. Lukacs, P. Haggie, O. Seksek, D. Lechardeur, N. Freeman, and A. S. Verkman, J. Biol. Chem. **275**, 1625 (2000).
[32] J. Kim, J. Lee, S. Hamada, S. Murata, and S. H. Park, Nat. Nanotechnol. **10**, 528 (2015).
[33] J. Valero, N. Pal, S. Dhakal, N. G. Walter, and M. Famulok, Nat. Nanotechnol. **13**, 496 (2018).
[34] M. Kim, S. Bae, I. Oh, J. Yoo, and J. S. Kim, Nanoscale **13**, 20186 (2021).
[35] M. Kim, C. C. Hong, S. Lee, and J. S. Kim, Bull. Kor. Chem. Soc. **43**, 523 (2022).